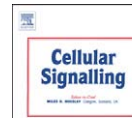




Contents lists available at ScienceDirect

Cellular Signalling

journal homepage: www.elsevier.com/locate/cellsig

A functional RNAi screen identifies hexokinase 1 as a modifier of type II apoptosis

Anja Schindler, Edan Foley*

Dept. of Medical Microbiology and Immunology, University of Alberta, Alberta Institute for Viral Immunology, Edmonton AB, Canada T6G 2S2

ARTICLE INFO

Article history:

Received 11 March 2010

Accepted 29 April 2010

Available online xxx

Keywords:

Apoptosis
Hexokinase 1
Caspase-8
DISC
TNF

ABSTRACT

Tumor necrosis factor alpha (TNF- α) signals through NF- κ B, JNK, and caspase modules to drive physiological responses that range from inflammation to apoptosis. The balance between the individual modules determines the nature of the response, and deregulated TNF signaling has been implicated in numerous pathological conditions. We used a quantitative high-throughput RNA interference assay to probe the entire complement of human kinases and phosphatases for gene products that tilt the balance of TNF signal transduction in favor of cell death or cell viability. Of all gene products tested, loss of hexokinase 1 resulted in the greatest elevations in TNF-dependent death. In secondary assays, we demonstrated that hexokinase 1 does not alter TNF-dependent activation of NF- κ B or JNK modules. Instead, hexokinase 1 modifies the induction of caspase-driven cell death. Specifically, we showed that hexokinase 1 inhibits the formation of active, pro-apoptotic caspases in response to extrinsic inducers of apoptosis. These data are the first loss-of-function reports to examine the involvement of hexokinase 1 in the transduction of cell death signals and indicate that hexokinases are critical determinants of the viability of cells in response to extrinsic apoptotic cues.

© 2010 Elsevier Inc. All rights reserved.

1. Introduction

Tumor Necrosis Factor alpha (TNF- α) drives critical inflammatory events and coordinates a range of physiological responses that includes differentiation, proliferation and cell death [1,2]. TNF signals through three conserved modules; an NF- κ B, a c-Jun N-terminal Kinase (JNK), and a caspase module [2,3]. While unchecked signal transduction through the JNK or caspase arms often results in apoptosis, NF- κ B mediates a dominant pro-survival response that includes the transcriptional induction of anti-apoptotic factors [1,4–7].

Within minutes of TNF detection, the TNF receptor activates NF- κ B through the assembly of a distinct molecular complex (complex I) at the plasma membrane [8]. The TNF Receptor-Associated Death Domain (TRADD), Receptor-Interacting Protein 1 (RIP1) and TNF Receptor-Associated Factor 2 (TRAF2) proteins are essential components of complex I [8]. Complex I activates the I κ -B Kinase (IKK) complex through association with and post-translational modification of the IKK subunit NEMO [9]. Active IKK then activates NF- κ B transcription factor family members by directing proteasomal destruction of the NF- κ B inhibitor, I- κ B [10,11]. Liberated NF- κ B dimers initiate transcription of more than two hundred distinct genes. Anti-apoptotic factors such as c-FLIP, Bcl-2 family members and Inhibitor of Apoptosis Proteins (IAPs) form a major subset of NF- κ B-responsive genes and are essential for inhibition of the apoptotic arm of the TNF pathway [4].

The pro-apoptotic component (complex II) forms approximately 2 h after the engagement of the TNF receptor upon internalization of TNF receptosomes. Complex II formation involves the recruitment of caspase-8 and the Fas-Associated Death Domain (FADD) adaptor molecule to RIP1, TRADD and TRAF2 [8,12–16]. Active complex II transduces extrinsic apoptotic signals to effector caspases such as caspase-3 and caspase-7. Researchers distinguish two classes of complex II-mediated apoptosis: type I apoptosis, where signal transduction proceeds directly from complex II to effector caspases; and type II apoptosis, where a mitochondrial amplification loop is required for activation of effector caspases [17]. The current model of type II apoptosis is that active caspase-8 cleaves cytosolic Bid to generate a pro-apoptotic tBid, which drives mitochondrial membrane permeabilization and release of pro-apoptotic factors such as cytochrome c from the mitochondria into the cytoplasm. In both forms of apoptosis, active effector caspases usher in the defining molecular and morphological features of apoptosis [18].

Deregulated signal transduction through the TNF pathway has devastating consequences for mammalian health. For example, TNF signaling has been implicated in autoimmune, neurological and cancerous disorders [2,19]. Thus, there is a clear need to identify the cellular components that coordinate interactions between the individual TNF signaling modules. We previously described a high-throughput platform for the identification of modifiers of TNF-dependent cell death in RNAi-based assays [20]. In this manuscript, we used this assay to probe all human phosphatases and kinases for regulators of cell death decisions by TNF.

In our survey of the human kinome, we identified hexokinase 1 (HK1) as a potent inhibitor of TNF-dependent cell death. HK1 is

* Corresponding author. Tel.: +1 780 492 2303; fax: +1 780 492 9828.
E-mail address: efoley@ualberta.ca (E. Foley).

primarily known for its role in the initiation of glycolysis through the phosphorylation of glucose. However, several recent studies implicated HK1 in the transduction of pro-survival signals in response to growth factors [21–25]. Molecular studies indicate that survival factors signal through AKT to induce a mitochondrial localization of the paralogous gene products HK1 and HK2. Mitochondrial hexokinases then contribute to the maintenance of mitochondrial integrity and cellular viability.

In contrast to our understanding of the role of HK1 in survival signaling, the involvement of HK1 in cellular responses to physiological inducers of apoptosis is almost entirely unexplored. In this study, we present the first detailed analysis of the consequences of HK1 depletion and demonstrate that loss of HK1 results in greatly enhanced cell death in response to a number of physiological inducers of apoptosis. In follow-up studies, we show that loss of HK1 accelerates the formation of active complex II upon induction of apoptosis and thereby accelerates the rate of entry into apoptosis. Given the established positive role of mitochondrial hexokinases in pro-survival signaling, our data raise the intriguing possibility that HK1 sits at the nexus of two diametrically opposed signal transduction pathways that ultimately determine the death or survival of a cell.

2. Materials and methods

2.1. Cell culture

HeLa cells were received from Dr. Michele Barry, HEK293T from Dr. Deborah Burshtyn, U2OS from Dr. James Smiley, A549 cells from Dr. Michael Weinfeld, HepG2 cells from Dr. Lorne Tyrrell, Raji cells from Dr. Hanne Ostergaard, BJAB cells from Dr. Robert Ingham (all University of Alberta, Edmonton, AB), and SKW6.4 cells a gift from Dr. Andreas Strasser (The Walter and Eliza Hall Institute of Medical Research, Australia). All cells were cultured at 37 °C and 5% CO₂. HeLa, HEK293T, U2OS, A549, and HepG2 cells were cultured in Dulbecco's modified Eagle Medium with 4.5 g/l D-glucose and L-glutamine (GIBCO) supplemented with 10% fetal bovine serum (GIBCO), 50 U/ml penicillin and 50 µg/ml streptomycin (GIBCO). Raji, SKW6.4, and BJAB cells were cultured in RPMI medium with 25 mM HEPES and L-glutamine (GIBCO) supplemented with 10% fetal bovine serum (GIBCO), 50 U/ml penicillin and 50 µg/ml streptomycin (GIBCO). The medium for SKW6.4 cells was further supplemented with 2 mM L-glutamine (GIBCO); the medium for BJAB cells was further supplemented with 2 mM L-glutamine (GIBCO), 1 mM sodium pyruvate (GIBCO), and β-Mercaptoethanol (Bioshop Inc.).

2.2. Cell treatments

HeLa cells were treated with 20 ng/ml TNF (Roche) and 5 µg/ml CHX (Sigma), or 200 ng/ml anti-Fas antibody CH-11 (Millipore), or 50 ng/ml recombinant TRAIL (PeproTech Inc.) to induce apoptosis, or 20 ng/ml TNF to induce NF-κB or JNK signaling. For the immunoprecipitation of complex II, HeLa cells were treated with 20 ng/ml TNF and 10 µg/ml CHX. HEK293T cells were treated with 20 ng/ml TNF. U2OS and A549 cells were treated with 20 ng/ml TNF and 10 µg/ml CHX.

2.3. siRNAs

The human kinase siRNA library V3 and human phosphatase siRNA library V3 (Applied Biosystems Life Technologies Corp.) were used in the screen. We used AllStars negative Control siRNA, caspase-8 siRNA (Qiagen), NEMO siRNA, c-FLIP siRNA, and TAB2 siRNA (all Applied Biosystems) as control siRNAs. Hexokinase was targeted with three non-overlapping siRNAs from Applied Biosystems and four non-overlapping siRNAs from Qiagen.

2.4. siRNA transfections

10 µl of a 200nM siRNA solution in water were spotted into each well of a 96 well plate. The siRNA was mixed with 15 µl transfection mix containing 0.2 µl Dharmafect 1 transfection reagent (Dharmacon) and 14.8 µl OptiMEM (GIBCO). 6500 HeLa cells in 75 µl antibiotic-free culture medium were added after 30 min. The final siRNA concentration was 20 nM. Cells were incubated for 72 h to allow protein depletion. For the transfection of U2OS cells, water and OptiMEM were replaced by DMEM (GIBCO); 0.375 µl HiPerfect (Qiagen) were used as a transfection reagent. 3000 cells were seeded into each well. For siRNA transfections in 12-well or 6-well plates, all volumes were scaled up by a factor of 10 or 20, respectively, and siRNAs were diluted in OptiMEM, instead of water. 7.8×10^4 HeLa cells, or 4875 U2OS cells, or 4875 A549 cells were seeded into 12-well plates, and 1.95×10^5 HeLa cells into 6-well plates. siRNA transfections for the NF-κB reporter assay were done in 384-well format. Per well, 5 µl of a 160 nM siRNA solution in OptiMEM were mixed and incubated with 5 µl OptiMEM containing 0.0875 µl Dharmafect 1 transfection reagent for 20 min. The mix was spotted into a well of the 384-well plate. 3500 HEK293T cells were added in 30 µl antibiotic-free culture medium and incubated for 48 h, prior to the second transfection with reporter plasmids. The final siRNA concentration was 20 nM.

2.5. Viability assay

Cells were treated with TNF and CHX for 13.5 h. A 440 µM resazurin sodium salt (Sigma) solution was added to a final concentration of 10% and incubated with the cells for an additional 1.5 h. Reduction of non-fluorescent resazurin into fluorescent resorufin by living cells was measured with an EnVision plate reader (PerkinElmer) using a 544 nm excitation filter and a 590 nm emission filter.

2.6. siRNA screen and data analysis

Each kinase or phosphatase was targeted with three distinct siRNAs. The source plate organization is outlined in Fig. 1a. Each source plate was transfected in quadruplicate. Two plates were treated with TNF/CHX and two were left untreated. Cell viability was measured as described above. Each viability value was normalized to the mean viability value of the non-silencing siRNA controls in the same plate. Viability values were then averaged for replicate plates. The mean viability values with and without treatment were used to determine the death index for each siRNA. The death index was defined as the ratio of the viability without TNF/CHX stimulation to the viability with

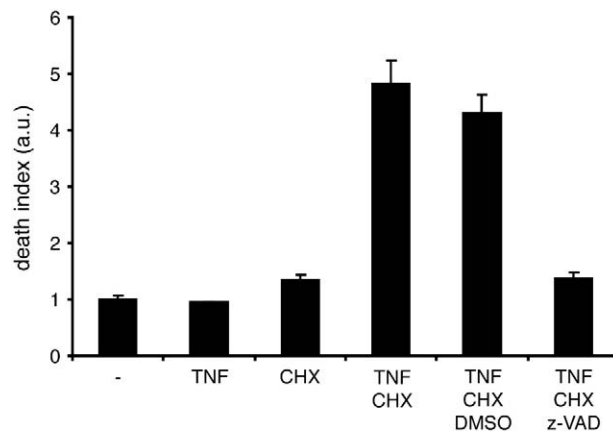


Fig. 1. The combined treatment with TNF and CHX induces cell death through a caspase-dependent mechanism. Representative death indices for HeLa cells (–), HeLa cells treated with TNF, cycloheximide (CHX), TNF and CHX, TNF, CHX and DMSO, or TNF, CHX and the pan-caspase inhibitor z-VAD-fmk in a resazurin viability assay.

TNF/CHX stimulation. These steps assign the non-silencing siRNA controls a death index of one. All genes were sorted according to their median siRNA death index. Due to an asymmetric distribution of pro-survival proteins (death index of greater than one) and pro-death proteins (death index smaller than one) we determined confidence intervals for pro-survival genes and pro-death genes independently. To this end, we determined the standard deviation of the median siRNA death indices from the non-silencing siRNA control for pro-survival and pro-death proteins. Genes with a median siRNA death index greater than 2.58 standard deviations from the non-silencing control belong in the 99% confidence interval group. Genes with a median siRNA death index greater than 1.96 standard deviations from the non-silencing control belong in the 95% confidence interval group.

2.7. Expression constructs

The NF- κ B reporter construct pNF- κ Bluc was provided by Dr. Michele Barry (University of Alberta, Edmonton, AB). The control reporter plasmid pRL-TK was obtained from Promega. cDNAs for HK1 and HK2 were purchased from Open Biosystems. HK1 cDNA was amplified with a forward primer containing a SacI restriction site and a reverse primer containing a PstI restriction site; HK2 cDNA was amplified with a forward primer containing a HindIII restriction site and a reverse primer containing an EcoRI restriction site. The PCR products were subcloned into the vector pEGFP-N1 (Invitrogen), to generate a C-terminally tagged HK1-GFP or HK2-GFP, respectively. The HK1-GFP construct was used as the template to generate the expression construct for inactive HK1S603A-GFP according to the Stratagene protocol for site directed mutagenesis. All constructs were verified for their respective sequence. Primer sequences are listed in [Supplemental Table 2](#).

2.8. Transfection of expression constructs

HeLa cells were plated into 12-well plates as 2×10^5 cells/well 1 day prior to transfection. For transfection, each well was washed once with $1 \times$ PBS, and the medium replaced with 250 μ l OptiMEM (GIBCO). 250 μ l transfection mix containing 1 μ g DNA in 125 μ l OptiMEM and 2 μ l Lipofectamine2000 (Invitrogen) in 125 μ l OptiMEM, mixed and incubated for 20 min, were added drop-wise. After 4 h, cells were recovered by the addition of 500 μ l DMEM (GIBCO) containing 20% fetal bovine serum.

2.9. Western blot

Approximately 8×10^5 cells were washed once in PBS and scraped into 50 μ l lysis buffer (20 mM Tris, pH 7.5, 25 mM Glycerol-3-phosphate, 150 mM NaCl, 1% Triton X-100, 2 mM Na_3VO_4 , protease inhibitors). The soluble fraction of the lysates was added to 80 μ l sample buffer (62.5 mM Tris, pH 6.8, 10% Glycerol, 2% SDS, 50 mM β -Mercaptoethanol, Bromophenol Blue) and boiled for 5 min. Proteins were separated by SDS-PAGE electrophoresis and transferred to a nitrocellulose membrane by semi-dry transfer. Membranes were blocked in blocking buffer (LI-COR Biosciences) and probed with rabbit anti-HK1 C35C4 (Cell Signaling), mouse anti-phospho-I κ B α (Ser32/36) 5A5 (Cell Signaling), mouse anti-PARP C2-10 (Trevigen Inc.), rabbit anti-FADD H-181 (Santa Cruz Biotechnology Inc.), mouse anti-caspase-8 1C12 (Cell Signaling), mouse anti-actin AC-40 (Sigma), or rabbit anti-pan-actin antibody (Cell Signaling). Secondary antibodies were Alexa Fluor 680 or 750 conjugated goat-anti-mouse or goat-anti rabbit IgG antibodies (Molecular Probes). Protein levels were detected with an Aeries automated imaging system (LI-COR Biosciences).

2.10. Quantitative real-time PCR

Total RNA was extracted from approximately 21×10^5 cells using Trizol (Invitrogen). cDNA was created using qScript cDNA SuperMix

(Quanta Biosciences). We monitored transcript amplification with Perfecta SYBR Green FastMix (Quanta Biosciences). Transcript expression levels were normalized to actin expression levels for each individual sample and to the normalized non-silencing control using the $\Delta\Delta\text{Ct}$ method.

2.11. NF- κ B reporter assay

3500 HEK293T cells per well of a 384-well plate were reverse transfected with siRNAs as described above. Each sample was set up in triplicate. After 48 h, the cells were transfected with an NF- κ B reporter plasmid pNF- κ Bluc and a control reporter pRL-TK. For this, 25 μ l of the siRNA transfection mix were aspirated and the remaining 15 μ l were supplemented with 10 μ l of a reporter transfection mix. The reporter transfection mix consisted of 1 μ g NF- κ B reporter pNF- κ Bluc and 0.1 μ g control reporter pRL-TK in 5 μ l OptiMEM (GIBCO) and 0.075 μ l Lipofectamine 2000 (Invitrogen) in 5 μ l OptiMEM, mixed and incubated for 20 min. After 6 h, cells were recovered with 10 μ l DMEM (GIBCO) containing 20% fetal bovine serum (GIBCO). 24 h after transfection of the reporter plasmids, cells were stimulated with TNF in 5 μ l DMEM supplemented with 10% fetal bovine serum for 9 h. Subsequently, 25 μ l of the culture medium in each well were aspirated, and a Dual Glo luminescence assay (Promega) was performed according to the manufacturer's instructions, with the exception of the use of half the recommended amount of STOP and Glo reagent. Luminescence derived from the NF- κ B-induced expression of Firefly luciferase (pNF- κ Bluc vector) or the constitutive expression of a thymidine kinase-dependent Renilla luciferase (pRL-TK vector) was measured with an EnVision plate reader (PerkinElmer) using the settings for ultrasensitive luminescence. Induced NF- κ B activity was calculated as the difference of the ratio of the Firefly luminescence to Renilla luminescence between TNF-stimulated and unstimulated samples.

2.12. In-cell Western

Cells were transfected with siRNAs and stimulated with TNF as described above. Cells were washed in PBS and fixed with 3.7% formaldehyde in PBS, washed and permeabilized in 0.1% Triton X in PBS and blocked in blocking buffer (LI-COR Biosciences). Cells were probed with rabbit anti-phospho-JNK pTgPy antibody (Promega) and washed with 0.1% tween-20 in PBS. p-JNK staining was detected with Alexa Fluor 750 conjugated goat-anti rabbit IgG antibody (Molecular Probes), and filamentous actin was stained with Alexa Fluor 680 conjugated phalloidin (Molecular Probes). Cells were washed in 0.1% tween-20 in PBS, and p-JNK and f-actin were quantified with an Aeries automated imaging system (LI-COR Biosciences) following the manufacturer's instructions.

2.13. TMRE assay

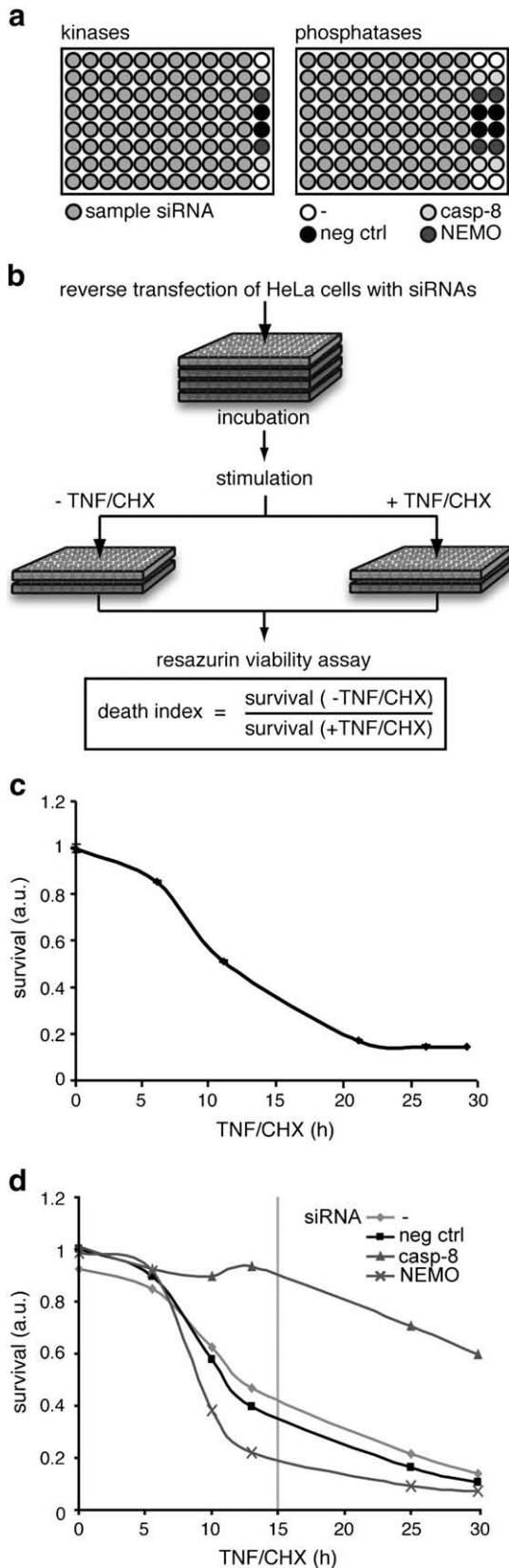
Cells were incubated with 1 μ M tetramethylrhodamine ethyl ester (TMRE; Molecular Probes) for 0.5 h. Cells were washed with PBS, harvested by trypsinization, and resuspended in PBS. The percentage of TMRE negative cells of the total population with a loss of the mitochondrial membrane potential was determined by flow cytometry (FACScan, Becton Dickinson). Data were acquired on 10,000 cells with fluorescence at logarithmic gain and analyzed with the CellQuest software.

2.14. Immunoprecipitation of complex II

HeLa cells were seeded and, where applicable, reverse transfected with siRNAs as described above. Around 15×10^6 cells per sample were treated with TNF and CHX, then harvested by trypsinization and lysed in 1 ml lysis buffer (20 mM HEPES pH = 7.5, 150 mM NaCl, 1% Triton X,

10% glycerol, 1 mM phenylmethylsulfonyl fluoride, and small peptide inhibitors). Lysates were cleared by centrifugation at $14,000 \times g$ at 4°C . Input samples were prepared from the supernatant. Remaining supernatant was rocked with 2 μg anti-FADD H-181 antibody (Santa

Cruz Biotechnology Inc.) O/N at 4°C . 40 μl Protein G-Sepharose 4B beads (Sigma) were added and rocked with the samples for 1 h at room temperature. Beads were precipitated by centrifugation at $500 \times g$ at 4°C , washed three times with 1 ml lysis buffer, supplemented with sample buffer (250 mM Tris, pH 6.8, 40% Glycerol, 8% SDS, 200 mM β -Mercaptoethanol, Bromophenol Blue), and boiled for 10 min. Western blots were prepared as described above. Input samples represent one fortieth of the immunoprecipitation.



2.15. Immunofluorescence

HeLa cells were plated onto round 25 mm glass cover slips (Fisherbrand) in a 6-well plate with a density of 3.5×10^5 cells/well and transfected with the HK1-GFP expression construct as described above. Cells were stained with MitoTracker Red 580 (Molecular Probes) at a concentration of 250 nM in culture medium for 0.5 h. Cells were washed once with culture medium, then transferred into CO_2 -independent Medium (GIBCO). Images were obtained at 37°C using a spinning disk confocal system (Ultraview ERS; Perkin Elmer, Norwalk, CT) equipped with a CS9100-50; camera (Hamamatsu, Bridgewater, NJ), and an Axiovert 200 M microscope (Carl Zeiss MicroImaging, Thornwood, NY) using Ultraview ERS software (Version 2, Perkin Elmer).

3. Results

3.1. A plate-based assay for TNF modifiers

We developed a plate-based assay to identify modifiers of TNF-mediated cell death. Specifically, we treated HeLa cells with siRNAs that target all human kinases and phosphatases and monitored the subsequent viability of cells treated with TNF and a sub-lethal dose of the translation inhibitor cycloheximide (CHX) in comparison to control cells that were not treated with TNF/CHX. We considered HeLa cells a suitable model for such studies, as they are accessible to automated RNAi screens and faithfully reproduce prominent features of signal transduction in response to TNF. The concentration of CHX used did not induce cell death, but was sufficient to induce widespread cell death in combination with TNF, presumably due to disrupted translation of TNF-responsive anti-apoptotic gene products (Fig. 1).

The organization of each siRNA plate is outlined in Fig. 2a. We assayed each siRNA in the presence or absence of TNF/CHX in duplicate and defined the death index for each siRNA as the ratio of cell viability for cells without TNF/CHX to cells treated with TNF/CHX (Fig. 2b). TNF/CHX treatment reproducibly resulted in a five-fold decrease in cell viability over 30 h (e.g. Fig. 2c). As anticipated, siRNA-mediated inactivation of the TNF pathway elements caspase-8 and NEMO suppressed and enhanced TNF-dependent cell death, respectively. For caspase-8 siRNA, cell viability was six-fold higher than in a population of control cells treated with a non-silencing siRNA 15 h

Fig. 2. An siRNA screen for modifiers of TNF-induced cell death. (a) The locations of sample and control siRNAs are shown for kinase and phosphatase siRNA plates. Control siRNAs targeted caspase-8, NEMO or were non-silencing (neg ctrl). (b) Flow chart of the siRNA screen. Each 96-well library plate was reverse transfected into HeLa cells in quadruplicate. Following a three-day incubation period, the cells in two of the four plates were treated with TNF/CHX to induce apoptosis, and the two remaining plates were left untreated. Cell viability was determined in a resazurin viability assay for each plate. TNF-induced cell death (death index) was determined as the ratio of the average viability without TNF/CHX treatment to the average viability with treatment. (c) Representative time course of the viability of HeLa cells treated with TNF/CHX. Viability was determined in a resazurin viability assay. (d) Representative time course of the viability of HeLa cells depleted of TNF signaling components and treated with TNF/CHX. Cells were depleted of caspase-8 (casp-8) or NEMO, respectively. Control cells were treated with a non-silencing control siRNA (neg ctrl) or no siRNA (-). Viability was determined in a resazurin viability assay.

after TNF/CHX exposure. Depletion of NEMO resulted in a two-fold increase of cell death fifteen hours after treatment with TNF/CHX compared to control cells treated with a non-silencing siRNA (Fig. 2d). From these data, we conclude that 15 h treatment with TNF/CHX is a suitable time point to identify siRNAs that enhance or suppress TNF-mediated cell death.

3.2. Identification of novel modifiers of TNF-induced cell death

We then screened the human kinome for siRNAs that modify TNF-induced cell death. A detailed analysis of our screen results is presented in Supplementary Table S1. We tested three non-overlapping siRNAs independently for each gene and we considered a gene a modifier if a minimum of two of three gene-specific siRNAs had a significantly altered death index in comparison to control non-silencing siRNAs. We then plotted the median siRNA death index for each gene relative to control non-silencing siRNAs and determined confidence intervals for enhancers and suppressors of TNF-induced cell death (Fig. 3a). We reasoned that depletion of pro-survival gene products will result in elevated death indices in cells treated with TNF/CHX, while loss of pro-death gene products will result in decreased death indices for cells treated with TNF/CHX. Consistent with this hypothesis, control siRNAs that targeted NEMO and caspase-8 belonged to the 99% confidence intervals for pro-survival or pro-death proteins, respectively. Furthermore, we identified the established pro-survival proteins TAB2 and NEMO and the pro-death protein JNK1 in the anticipated groups with high confidence (Fig. 3a). We then analyzed the primary screen data to determine the phenotypes of additional TNF pathway components. We found that elements of the NF- κ B arm clustered as pro-survival proteins, while members of the AP-1 and caspase arms clustered as pro-death proteins (Fig. 3b). These phenotypes are in line with the established roles of the NF- κ B, JNK and caspase modules in the regulation of TNF-responsive cell death. Proteins with partial redundancies such as IKK α and IKK β appeared in lower confidence intervals than non-redundant proteins such as RIP1, TAB2 and NEMO. These data indicate that our assay is suitable for the identification of new modifiers of TNF-mediated death.

Of the approximately one thousand genes examined, hexokinase 1 (HK1) had the strongest pro-survival phenotype (Fig. 3a). All three HK1 siRNAs produced phenotypes comparable to the pro-survival protein NEMO and suggest that HK1 has essential pro-survival functions in the TNF pathway (Fig. 3c). The pro-survival function appears specific to the HK1 isoform as siRNAs that target HK2, HK3 or HK4 had negligible impacts on cell viability. We do not believe that the phenotype is an indirect consequence of HK1 loss on general cell viability, as the siRNAs alone did not alter cell viability in the absence of TNF/CHX (Fig. 3d). Furthermore, loss of HK1 did not result in apparent declines in total cellular ATP levels (data not shown). Likewise, the enhanced cell death observed upon HK1 depletion is not an indirect consequence of exposure to CHX, as a combined HK1 siRNA/CHX regime had minimal effects on cell viability (Fig. 4b). These data suggest that HK1 specifically modifies TNF-responsive cell death.

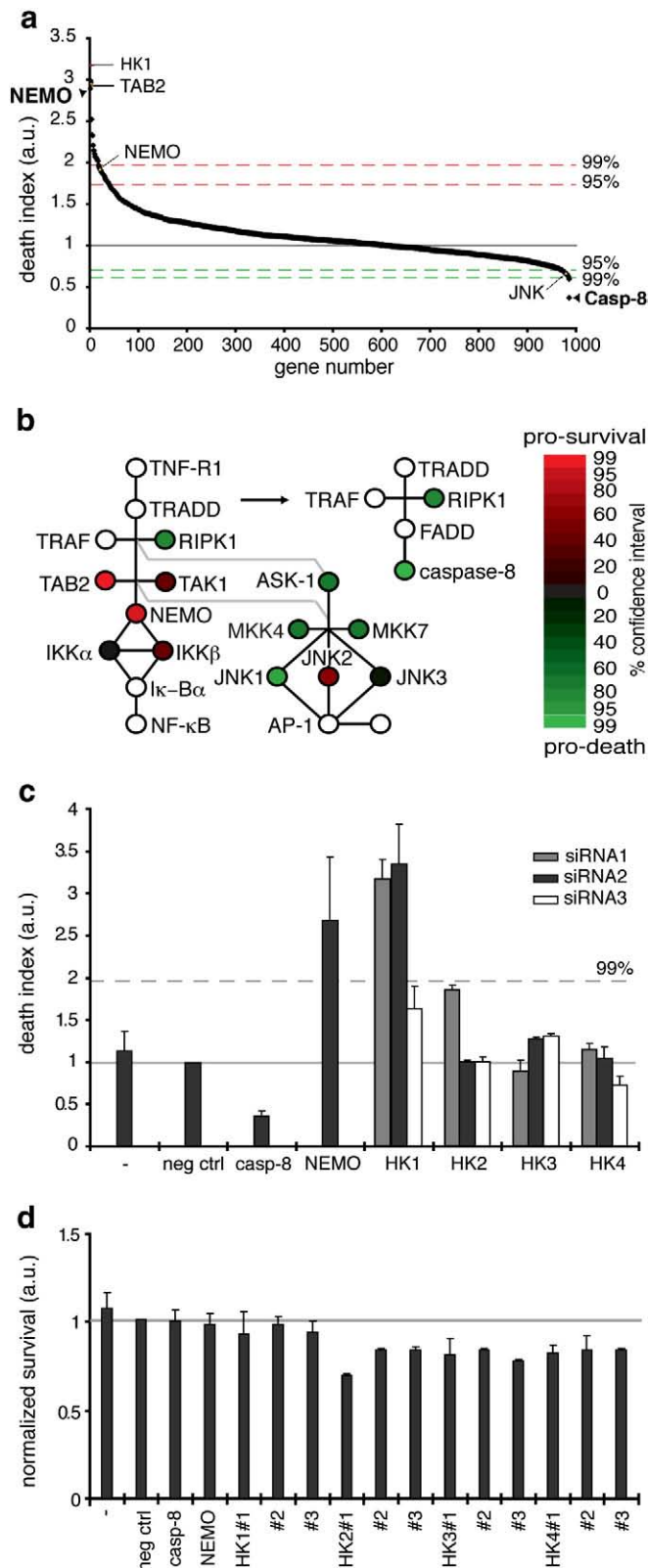
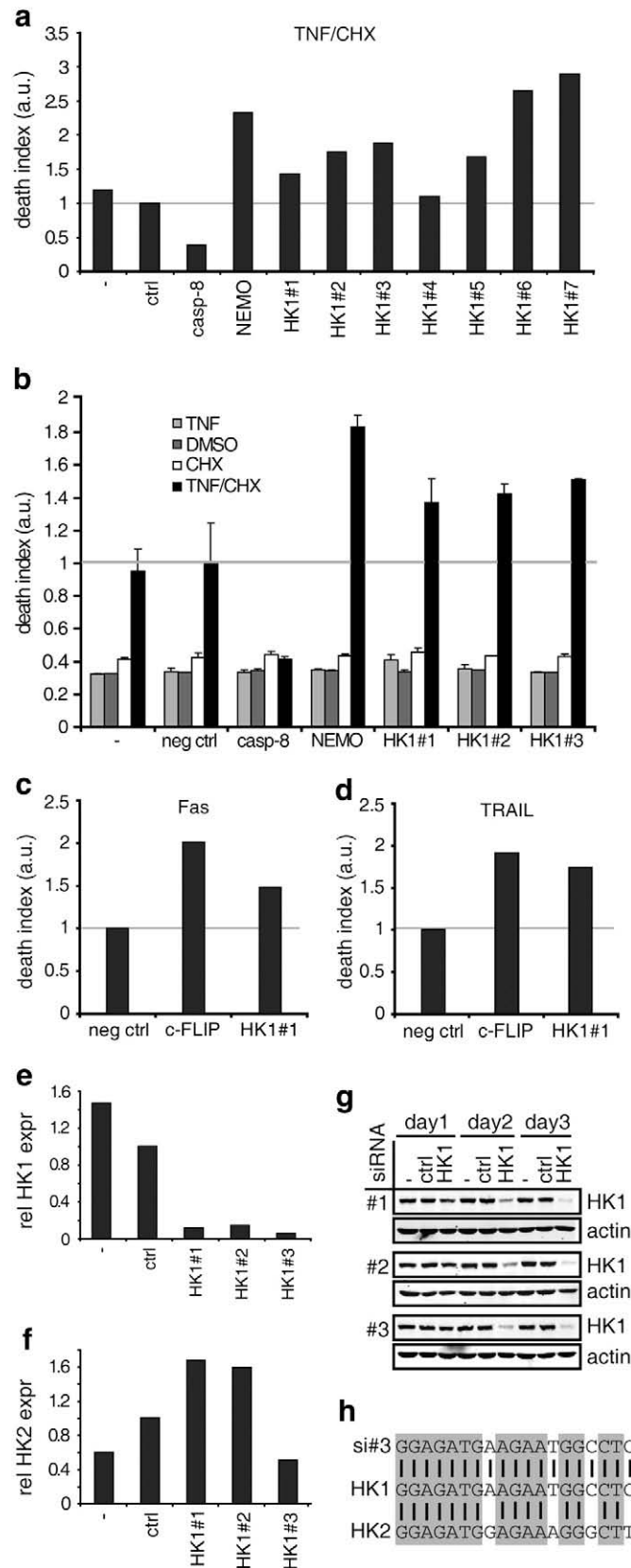


Fig. 3. Identification of TNF signaling modifiers. (a) Distribution of the median siRNA death index per gene from the screen. The median siRNA death index for each gene was sorted in descending order. 99% and 95% confidence intervals are indicated for enhancers and suppressors of cell death. The average death index of control cells treated with siRNAs that target NEMO or caspase-8 are indicated. Median siRNA death indices for TAB2, NEMO and JNK1 are indicated. (b) Graphic representation of the TNF pathway interaction network. Genes tested in the screen are indicated with colored circles. The color of the circle represents the pro-death or pro-survival confidence interval value for the respective gene. (c) Death indices of all four hexokinase (HK) isoforms in the siRNA screen. The average death index for each siRNA tested is shown. All death indices are normalized to the death index of cells treated with a non-silencing control siRNA (neg ctrl) indicated by a solid line. The death indices of control cells treated with an siRNA against caspase-8 (casp-8), NEMO or no siRNA (–) are shown as the average value + S.E.M. from all screen plates. The dashed line indicates the 99% confidence interval. (d) Normalized cell viability for each HK1 isoform siRNA in the absence of TNF/CHX treatment. The viability of cells treated with non-silencing siRNA (neg ctrl) was assigned a value of one for each experimental condition, and all other values are reported relative to that value.

3.3. Hexokinase inhibits TNF-induced cell death

To validate HK1 as a pro-survival gene product, we retested the three HK1 siRNAs from the screen in addition to four independent HK1-specific siRNAs for their impacts on TNF-induced cell death. Six

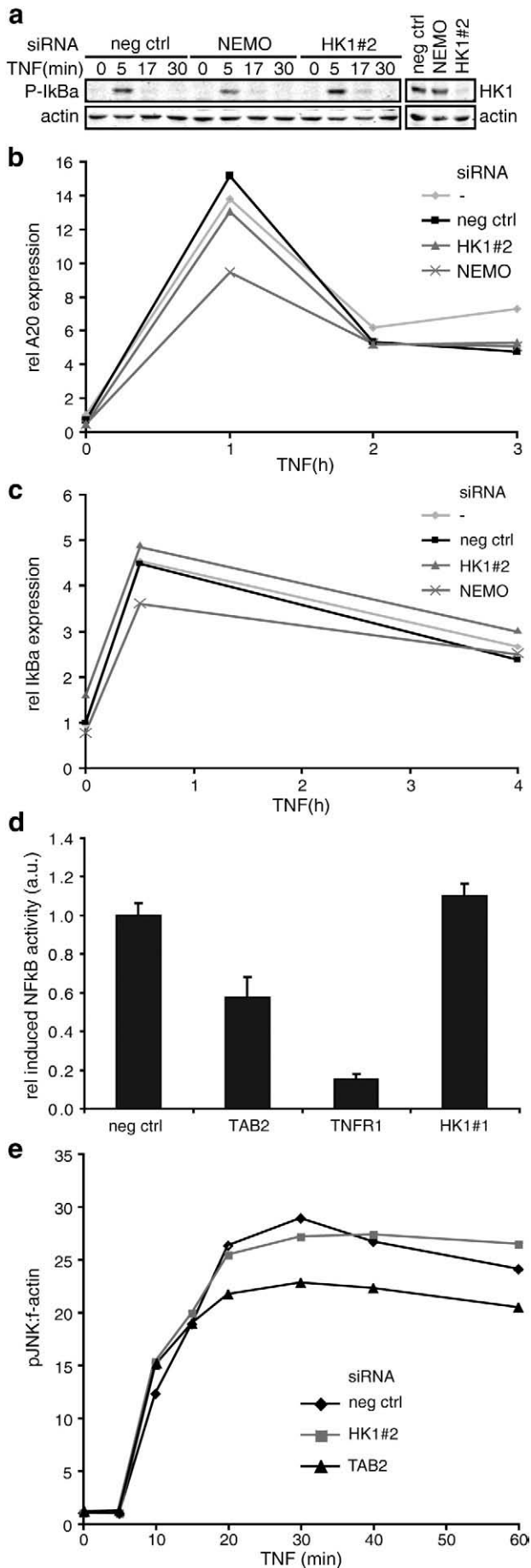


of the seven siRNAs led to clearly increased death indices (Fig. 4a). In several cases, the death indices were comparable to or higher than that observed for NEMO siRNA. Thus, we conclude that loss of HK1 greatly elevates TNF-responsive cell death in HeLa cells. We do not believe that interactions between HK1 and the apoptotic machinery are restricted to TNF responses, as we noticed similar effects for HK1 depletion on additional extrinsic apoptosis signals such as Fas ligand or TRAIL (Fig. 4c, d). To confirm that the HK1 siRNAs effectively targeted HK1, we treated cells with three different siRNAs and monitored the relative expression of HK1 by quantitative real-time PCR and Western blot analysis. All three HK1 siRNAs from the screen caused a strong reduction in HK1 transcript levels (Fig. 4e) and HK1 protein levels (Fig. 4g) after a three-day incubation period. As HK1 and HK2 are paralogs, we tested whether the phenotype ascribed to HK1 may result from a parallel, off-target depletion of HK2. To this end, we measured the levels of HK2 transcripts in cells treated with three different species of HK1 siRNA. Of the three siRNAs examined, only siRNA#3 also interfered with the expression of HK2 (Fig. 4f). We consider the parallel knockdown of HK2 likely an off-target effect, as siRNA#3 shares a significant sequence similarity with HK2 (Fig. 4h). In combination, our data strongly argue that loss of HK1 greatly increases the sensitivity of HeLa cells to extrinsic inducers of apoptotic death.

3.4. Hexokinase 1 does not modify TNF-induced NF-κB or JNK activation

We next sought to identify the point at which HK1 interacts with the TNF pathway. Given that HK1 performs a pro-survival function within the pathway, we reasoned that HK1 may be a positive regulator of NF-κB pro-survival signaling or a negative regulator of JNK or caspase pro-apoptotic signaling. We first characterized the consequences of HK1 loss for the NF-κB and JNK arms of the TNF pathway. We examined the effect of HK1 depletion on TNF-induced NF-κB signaling by depleting HK1 and monitoring several classical features of NF-κB activation. We initially examined the effect of HK1 loss on I-κBα phosphorylation. Exposure to TNF typically results in a rapid transitory phosphorylation of I-κBα (Fig. 5a). As expected, loss of NEMO reduced the extent of I-κBα phosphorylation. In contrast, depletion of HK1 did not affect I-κBα phosphorylation (Fig. 5a). Likewise, whereas depletion of NEMO diminished the expression of the NF-κB-responsive transcripts A20 and I-κBα, loss of HK1 did not alter A20 or I-κBα expression (Fig. 5b, c). Finally, loss of the TNF

Fig. 4. Confirmation of HK1 as an inhibitor of death receptor-induced cell death. (a) Death indices of cells depleted of HK1 and treated with TNF and CHX. siRNAs #1 to #3 were used in the screen, #4 to #7 are independent. Death indices were determined in a resazurin viability assay and are reported relative to the death index of cells treated with a non-silencing siRNA (ctrl). Control cells were treated with an siRNA against caspase-8 (casp-8), NEMO, or no siRNA (-). Data are representative of three independent experiments. (b) Death indices of HeLa cells depleted of HK1, NEMO, or caspase-8 (casp-8) and treated with TNF, CHX, the CHX solvent DMSO, or TNF and CHX. Death indices were determined in a resazurin viability assay. All death indices are reported as the mean + S.E.M. of two independent experiments and relative to the death index of cells treated with a non-silencing siRNA (neg ctrl) and DMSO. The death index of cells treated with a non-silencing siRNA and TNF/CHX was assigned a value of one. The apoptotic phenotype of HK1 depletion upon treatment with TNF and CHX is TNF-dependent. (c-d) Death indices of cells depleted of HK1 and treated with an anti-Fas antibody (c) or recombinant TRAIL (d). Death indices were determined in a resazurin viability assay and are reported relative to the death index of cells treated with a non-silencing siRNA (neg ctrl). Control cells were treated with an siRNA against c-FLIP. Data are representative of three independent experiments. In both assays, depletion of HK1 enhances cell death. Relative HK1 (e) or HK2 (f) expression levels in cells treated with HK1 siRNAs #1 to #3 as determined by quantitative real-time PCR. All values are normalized to the HK expression level in cells treated with a non-silencing control siRNA (ctrl). (g) Representative Western blot of the time course of HK1 expression in cells treated with HK1 siRNAs #1 to #3. For each day, cells were treated with an siRNA against HK1, a non-silencing control siRNA (ctrl), or no siRNA (-). Actin served as a loading control. (h) Sequence alignment between HK1 siRNA#3 (si#3), HK1 target sequence and HK2 off-target sequence. Identical nucleotides are highlighted in grey.



receptor or the TNF adaptor TAB2 resulted in decreased NF-κB reporter activity, whereas NF-κB reporter activity was indistinguishable in control cells and cells treated with HK1 siRNA (Fig. 4d). In combination, these data strongly suggest that HK1 loss does not negatively affect the NF-κB pathway.

We then asked whether loss of HK1 altered TNF-mediated activation of JNK. In these experiments, we monitored JNK activation in a plate-based immunofluorescence assay. The assay is a modification of a protocol we described previously for the quantification of JNK activation in the innate immune response of *Drosophila* S2 cells [26,27]. Specifically, we used monoclonal antibodies to quantify the extent of JNK phosphorylation in control cells, cells treated with HK1 siRNA and cells treated with TAB2 siRNA. We observed a robust TNF-responsive phosphorylation of JNK in HeLa cells treated with a control non-silencing siRNA. As anticipated, depletion of the TNF pathway adaptor protein TAB2 reduced TNF-responsive JNK activation at all time points (Fig. 5e). In contrast, loss of HK1 did not prevent the activation of JNK by TNF. In combination, these data suggest that HK1 loss does not result in gross alterations to signal transduction through the NF-κB and JNK arms of the TNF pathway.

3.5. Hexokinase 1 inhibits TNF-dependent apoptosis

While our secondary analysis indicated that HK1 does not interact with the JNK or NF-κB modules of the TNF pathway, depletion of caspase-8 completely reverted the enhanced cell death seen upon loss of HK1 (Fig. 6a, b). These data indicate an interaction between HK1 and caspase-mediated apoptotic events. To explore this link further, we characterized the consequences of HK1 loss for progression through apoptosis. We initially examined the effect of HK1 depletion on two features of caspase-mediated apoptosis; cleavage of the caspase substrate Poly [ADP-ribose] polymerase (PARP) and loss of the mitochondrial transmembrane potential. Depletion of HK1 with each one of three independent siRNAs resulted in accelerated PARP cleavage (Fig. 6c) upon exposure to TNF/CHX. In each case, depletion of HK1 essentially mirrored the accelerated PARP cleavage observed upon depletion of NEMO. The apoptotic phenotype observed for HK1 loss is not restricted to HeLa cells, as we detected similar phenotypes in the U2OS osteosarcoma cell line and the A549 lung carcinoma cell line (Fig. 6d–f). Likewise, HK1 loss led to an accelerated loss of the mitochondrial transmembrane potential for each siRNA tested (Fig. 6g).

We then examined the consequences of HK1 overexpression on the induction of cell death. We consistently detected a reduction in

Fig. 5. HK1 does not modify TNF-induced NF-κB or JNK signaling. (a) Western blot of the time course of I-κBα phosphorylation following TNF stimulation. HeLa cells were treated with siRNAs against HK1 or NEMO, or a non-silencing siRNA (neg ctrl) and then stimulated with TNF for the indicated time periods. The Western blot to the right shows the respective HK1 levels for the three siRNA treatments in unstimulated cells. Actin served as a loading control. (b–c) Time course of the relative expression of A20 (b) or I-κBα (c) following TNF stimulation. HeLa cells were treated with siRNAs that target HK1 or NEMO, a non-silencing siRNA (neg ctrl), or no siRNA (–) and then stimulated with TNF for the indicated time periods. All values are reported relative to the A20 or I-κBα expression in unstimulated cells treated with a non-silencing control siRNA. RNA from two independent experiments was pooled for quantitative real-time PCR. (d) Quantification of the TNF-induced transcriptional activity of NF-κB in an NF-κB reporter assay. NF-κB activity is presented as the luminescence derived from the luciferase expression of an NF-κB reporter relative to a control reporter. HEK293T cells were depleted of HK1, the TNF receptor TNFR1, TAB2, or treated with a non-silencing siRNA (neg ctrl) prior to TNF stimulation. NF-κB activities from a representative experiment are shown as the mean luminescence + S.E.M. of three parallel measurements. All values are reported relative to the NF-κB activity of cells treated with a non-silencing siRNA. (e) Quantification of an in-plate Western assay visualizing the time course of TNF-induced JNK phosphorylation. JNK phosphorylation is presented as the relative level of phosphorylated JNK (p-JNK) to the level of filamentous actin (f-actin) in a single well. HeLa cells treated with HK1, TAB2, or non-silencing siRNA were stimulated with TNF for the indicated time periods. The JNK phosphorylation in unstimulated cells treated with a non-silencing siRNA was assigned a value of one, and all other values are reported relative to that value.

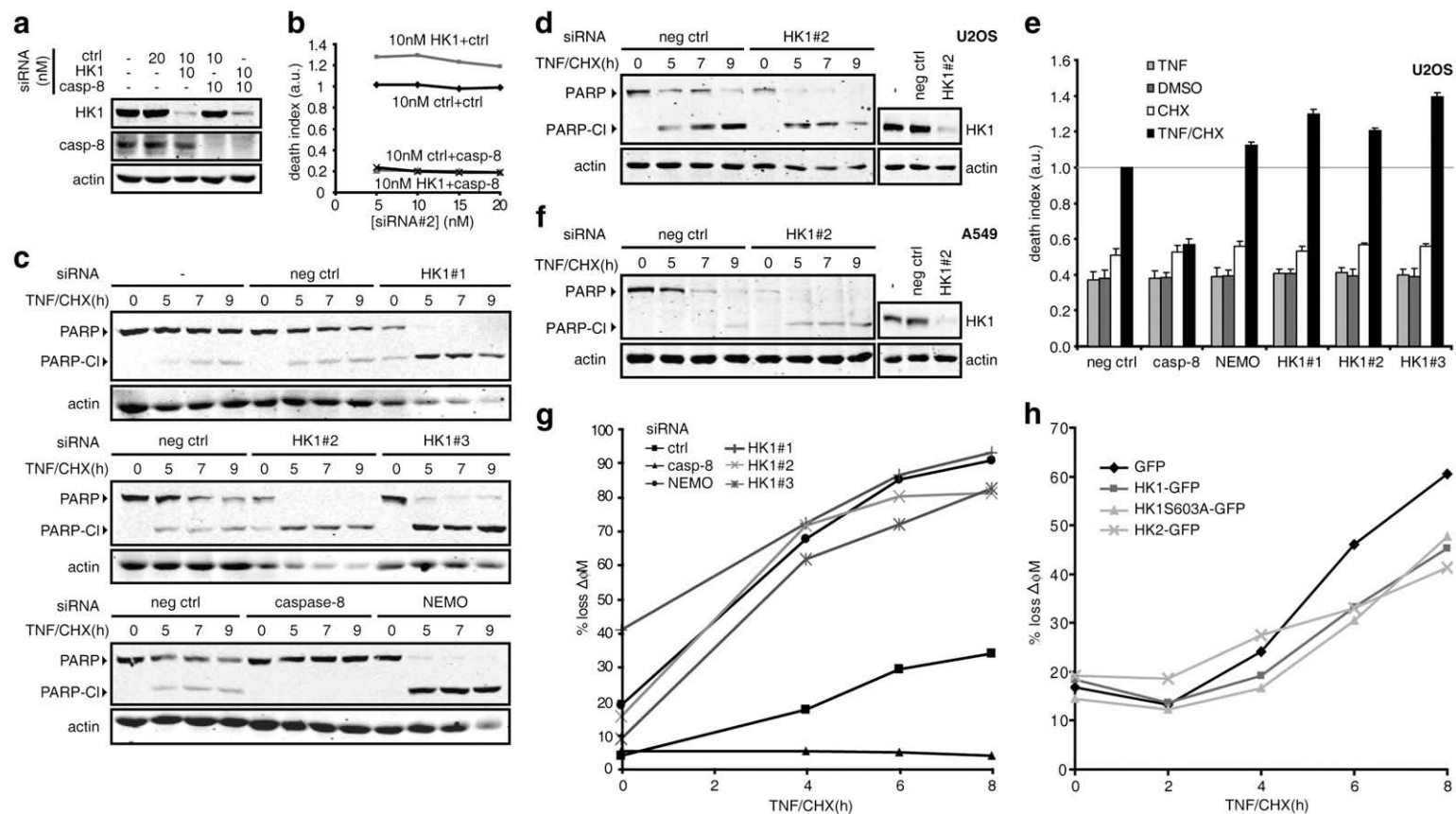


Fig. 6. HK1 inhibits TNF-induced apoptosis. (a) Representative Western blot of the expression of HK1 and caspase-8 in cells treated with siRNAs that target HK1 and/or caspase-8. Control cells were treated with a non-silencing siRNA (ctrl). Actin served as a loading control. (b) Representative death indices of cells depleted of HK1, caspase-8 (casp-8), or both. Each graph represents the death indices of cells treated with a constant concentration (10 nM) of a primary siRNA1 and four different concentrations (5–20 nM) of a secondary siRNA2. A non-silencing control siRNA (ctrl) was used to keep the total siRNA concentration in each sample constant. (c) Representative Western blot of the time course of PARP cleavage (into PARP-C1) following treatment with TNF/CHX. HeLa cells were treated with three different siRNAs against HK1, an siRNA against caspase-8 or NEMO, a non-silencing siRNA (neg ctrl), or no siRNA. Actin served as a loading control. (d) A representative time course of PARP cleavage following TNF/CHX treatment in U2OS cells. Cells were treated with a siRNA against HK1 or a non-silencing siRNA. The Western blot to the right shows the respective HK1 levels for the two siRNA treatments in unstimulated cells. Actin served as a loading control. (e) Death indices of U2OS cells depleted of HK1, NEMO, or caspase-8 and treated with TNF, CHX DMSO, or TNF and CHX. Death indices were determined in a resazurin viability assay. All death indices are reported as the mean + S.E.M. of two independent experiments and relative to the death index of cells treated with a non-silencing siRNA (neg ctrl) and TNF/CHX. (f) As in (d), but for A549 cells. (g) Time course of the loss of the mitochondrial membrane potential following treatment with TNF/CHX. All values are presented as the absolute percentage of TMRE negative cells in a cell population that was treated with one of three siRNAs against HK1, an siRNA against caspase-8 or NEMO, a non-silencing siRNA, or no siRNA. Representative of three independent experiments. (h) Time course of the loss of the mitochondrial membrane potential following treatment with TNF/CHX. All values are presented as the absolute percentage of TMRE negative and GFP-positive cells in a cell population that was transiently transfected with HK1-GFP, inactive HK1S603A-GFP, HK2-GFP, or a control GFP expression construct. Representative of six independent experiments.

TNF-dependent apoptotic levels upon overexpression of HK1 (Fig. 6h). The ability of HK1 to reduce apoptotic levels does not depend on the catalytic activity of HK1, as expression of a catalytically inactive HK1 variant (HK1S603A) also dampened the induction of apoptosis (Fig. 6h). We detected a similar effect upon expression of HK2 – a considerable reduction in the level of TNF-dependent cell death. We consider functional overlaps between HK1 and HK2 quite likely given the high degree of identity between the two proteins (73% identity). Quantitative PCR studies showed that HK1 expression levels are approximately eight fold higher in HeLa cells than HK2 expression levels, explaining the more pronounced cell death phenotype associated with HK1 depletion. In summary, depletion of HK1 accelerates progression through apoptosis while overexpression of HK1 decreases the rate of TNF-dependent cell death. These data argue that HK1 inhibits TNF-dependent progression through the apoptotic program.

3.6. Hexokinase I antagonizes caspase-8-dependent apoptosis triggered by TNF

Given the genetic interactions between HK1 and caspase-8, the accelerated apoptosis observed upon HK1 depletion and the decreased apoptosis observed upon HK1 overexpression, we reasoned that HK1 inhibits TNF-dependent apoptosis. HK1 has an N-terminal mitochondrial localization signal and fluorescence microscopy studies confirmed that HK1 is a mitochondrial protein in HeLa cells (Fig. 7a), suggesting that HK1 disrupts the mitochondrial step of TNF-mediated cell death. This contention is supported by our observation that depletion of HK1 alone results in a loss of mitochondrial membrane permeability in the absence of any pro-apoptotic signal (e.g. Fig. 6g). These observations led us to examine the consequences of HK1 loss for complex II formation, a cellular event that requires mitochondrial amplification in response to TNF. Repeat complex II immunoprecipitation studies demonstrated that HK1 does not form a molecular complex with the DISC (e.g. Fig. 7b). Loss of HK1 consistently resulted in accelerated processing of caspase-8 to the mature active isoforms, indicating that HK1 blocks the formation of active caspase-8 complexes (Fig. 7c). Direct examination of DISC formation revealed that loss of HK1 caused an increased and accelerated formation of a mature, active complex II (Fig. 7d). These data strongly indicate that HK1 disrupts TNF-dependent complex II formation and thereby inhibits the induction of apoptosis. Given the mitochondrial localization of HK1 and the lack of direct interactions between HK1 and complex II, we consider it most likely that HK1 disrupts the mitochondrial amplification step in complex II formation.

4. Discussion

TNF regulates physiological events that include inflammation, induction of secondary immune responses and apoptosis [2]. Disruptions to these finely coordinated cellular events result in potentially lethal pathological conditions [2]. Here, we present the first systematic siRNA screen for modifiers of TNF-dependent cell death. Given the central role of NF- κ B and caspase family members in the fate of cancerous lesions [4,28–30], we chose to focus on the identification of modifiers of TNF-dependent cell death. We specifically surveyed all human kinases and phosphatases for gene products that determine the ability of TNF to induce cell death, as we consider such gene products ideal pharmacological targets. Our survey identified known and novel gene products as regulators of TNF-mediated cell death. We believe that these data come at a timely point in TNF research and will be of considerable interest to a large community of TNF and apoptosis researchers.

Reliable scoring criteria are essential for the accurate identification of TNF modifiers in unbiased siRNA screens. To minimize the impact of off-target effects (OTE, [31,32]) on our data analysis, we tested three

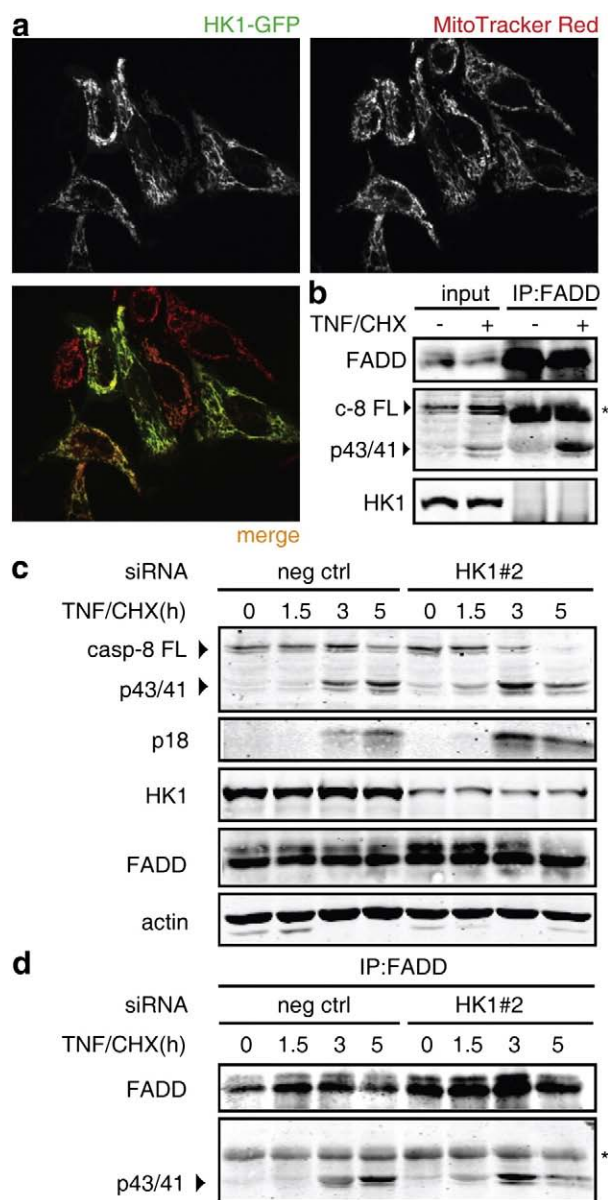


Fig. 7. HK1 antagonizes caspase-8 dependent apoptosis triggered by TNF. (a) Fluorescence microscopy of HeLa cells that were transiently transfected with a HK1-GFP expression construct and stained with mitotracker red. The intracellular localization of HK1-GFP is shown in the upper left panel and the localization of the mitochondria in the upper right panel. Both images were false-colored (HK1-GFP in green and mitotracker red in red) and merged (lower panel). (b) Representative Western blot of the immunoprecipitation of complex II. Complex II was precipitated with an anti-FADD antibody from lysates of untreated HeLa cells (–), or cells treated with TNF/CHX for 5 h (+). Original lysates (input) and precipitates (IP:FADD) were probed with an anti-FADD, anti-caspase-8 (casp-8), and anti-HK1 antibody on a Western blot. Caspase-8 is shown as the full-length caspase-8 (casp-8 FL) and p43/41 cleavage product. Unspecific signals from antibody heavy chains are labeled with *. (c) Representative Western blot of the time course of caspase-8 cleavage from full-length caspase-8 (casp-8 FL) into p43/p41 and p18 variants following treatment with TNF/CHX for the indicated time periods. Cells were treated with siRNAs that target HK1, NEMO or a non-silencing siRNA (neg ctrl) as indicated. FADD levels are constant. Actin served as a loading control. (d) Representative Western blot of the time course of complex II formation in HeLa cells depleted of HK1 or treated with a non-silencing siRNA (neg ctrl). Cell lysates for both siRNA treatments shown in (c) were precipitated for complex II with an anti-FADD antibody (IP:FADD). Each sample was probed with an anti-FADD and anti-caspase-8 (p43/41) antibody on a Western blot. Unspecific signals from antibody heavy chains are labeled with *. (For interpretation of the references to color in this figure legend, the reader is referred to the web version of this article.)

non-overlapping siRNAs independently for each target gene in duplicate. We then determined the death index for each siRNA and ranked the median siRNA death index for each gene from highest to lowest.

This method allowed us to group siRNAs into confidence intervals as pro-survival or pro-death gene products. As we scored confidence intervals for the median siRNA value for each gene, our evaluation criteria ensure that a minimum of two of the three siRNAs fall within the respective confidence intervals and thereby minimize the risk of OTE-directed false positive selection. We also tested each siRNA in duplicate in the presence or absence of the TNF/CHX regime. As an overwhelming majority of the siRNAs yielded reproducible phenotypes (Supplementary Fig. S1) we are confident in the phenotypes attributed to the respective siRNAs.

A comparison of anticipated hits with actual hits gives an approximate sense of the extent to which false negatives impair interpretation of the primary screen data. In our case, we reliably identified core TNF pathway members such as NEMO, TAB2 and JNK1 as critical modifiers of cellular responses to TNF. In fact, the mean death index for the NEMO control siRNA was almost identical to the death index attributed to the corresponding siRNA in the screen (Supplementary Fig. S2). Furthermore, we note that we successfully identified additional TNF pathway elements (e.g. RIP1, MKK4, and MKK7) as modifiers of TNF signal transduction. Thus, we are confident that the hit selection criteria applied in the primary screen permit identification of core TNF pathway elements. As a caveat, we note that our screen did not saturate the entire TNF pathway. For example, our primary data did not implicate the IKK α or β subunits as essential modifiers of the TNF pathway. Such deficiencies are inherent to large scale RNAi screens and likely occur through inefficient target knockdown or functional redundancies within the cell.

We were particularly intrigued by our identification of HK1 as a pro-survival gene product. Of the nine hundred eighty-six gene products tested, HK1 had the strongest pro-survival phenotype and we observed overlapping results for six of seven independent HK1 siRNAs in secondary evaluation. These results are strong indicators that HK1 is a potent inhibitor of the ability of TNF to induce cell death. Importantly, interactions between HK1 and the apoptotic machinery are not restricted to a single cell line, or a single inducer, as we observed parallel HK1 siRNA phenotypes in different cell lines and with different activators of extrinsic apoptosis. We do not believe that the death observed upon HK1 loss is the result of a general metabolic weakness, as HK1 depletion alone minimally increases death levels among HeLa cells and a combined HK1 siRNA/CHX treatment likewise had a minimal impact on cell viability. Importantly, we found that parallel depletion of caspase-8 completely reverted the increased cell death observed upon HK1 depletion the loss of HK1. In combination, these data strongly argue that HK1 specifically blocks caspase-8 dependent cell death in response to TNF.

We considered several possible explanations for the elevated death observed upon HK1 depletion: decreased activation of the NF- κ B module or elevated activation of the JNK or caspase modules. Our secondary analyses demonstrated that NF- κ B and JNK signaling are not altered by loss of HK1. In contrast, depletion of HK1 resulted in accelerated PARP cleavage, accelerated caspase-8 cleavage, elevated loss of mitochondrial transmembrane potential and accelerated complex II formation – four distinct hallmarks of caspase-dependent apoptosis. These data suggest that HK1 is a specific inhibitor of apoptotic events in response to TNF.

Hexokinase catalyzes the phosphorylation of glucose in glycolysis. The human genome encodes four hexokinase isoforms. HK1 and the structurally related HK2 have N-terminal mitochondrial localization sequences and preferentially use mitochondrial ATP for glucose phosphorylation. Interestingly, HK1 and HK2 expression is increased in many forms of cancer and mitochondrial hexokinases are central to the aerobic glycolysis (the Warburg effect) observed in many cancer types. At first glance, it appears counterintuitive that rapidly proliferating tumors prefer the comparatively inefficient glycolysis as a source of ATP generation, but a recent review speculated that aerobic glycolysis may be better suited to provide the metabolic

building blocks required to facilitate the accumulation of biomass in growing cancers [33]. Based on our findings and those of others, we speculate that HK1 may perform two additional non-enzymatic functions that contribute to tumor proliferation. Several recent studies uncovered a role for HK1 and HK2 in the transmission of pro-survival signals in response to growth factors [21–25]. These observations raise the possibility that mitochondrial hexokinases enhance the proliferation of tumors in response to extrinsic or tumor-derived growth factors. Given the involvement of apoptosis in the elimination of oncogenic lesions, we believe that our findings may uncover a third role for HK1 in governing tumor proliferation – namely in the attenuation of cancerous cell responses to innate and adaptive apoptotic defenses against tumor proliferation.

A recent study demonstrated that displacement of HK2 from isolated mitochondria with an artificial peptide resulted in an enhanced release of cytochrome *c* upon treatment with recombinant tBid [34]. While such studies support a general role for mitochondrial hexokinases in the inhibition of apoptotic signals, there is a paucity of studies that directly examine the cellular consequences of HK1 loss-of-function phenotypes. Furthermore, the involvement of HK1 in the transmission of apoptotic signals in response to physiological inducers of apoptosis is unexplored. In this study, we present the first direct examination of the consequences of the targeted deletion of HK1 for the transmission of pro-apoptotic signals. Our studies show that loss of HK1 results in accelerated formation of a mature DISC and a parallel acceleration of TNF-mediated apoptosis.

As HK1 is a mitochondrial protein that disrupts complex II formation without directly associating with complex II, we consider it most likely that HK1 acts by disrupting the mitochondrial amplification loop in the transmission of type II apoptotic signals. Consistent with this hypothesis, we did not observe HK1 expression in two (SKW6.4 and HepG2) of four type I apoptotic cells tested (Supplementary Fig. S3). These data indicate that type I apoptotic cells do not face the same selective pressures as type II apoptotic cells to increase the expression of HK1. Future HK1 loss-of-function studies are required to completely evaluate the contribution of HK to the transmission of type I apoptotic signals.

Hexokinase I and II reversibly associate with the outer mitochondrial membrane through an N-terminal localization sequence and growth factor signaling typically promotes hexokinase-mitochondria associations [21,23,24,35,36]. Our preliminary studies suggest that HK1 is not a TNF-induced transcript and that TNF does not alter association of HK1 with the mitochondrion (data not shown). It is generally accepted that pro-survival factors act through mitochondrial hexokinases to prevent the release of apoptogenic factors such as cytochrome *c* and thereby prevent the initiation of apoptosis [23]. In line with this hypothesis, we detected increased mitochondrial membrane permeability in cells that lack HK1. The mechanistic details of how mitochondrial hexokinases block cytochrome *c* release are unclear. There are two potentially non-exclusive hypotheses to explain hexokinase-mediated inhibition of apoptosis. In one scenario, hexokinase prevents the mitochondrial association of pro-apoptotic BH-3 only proteins and thereby inhibits the release of cytochrome *c* [37]. In a second model, hexokinase directly prevents the opening of the mitochondrial permeability transition pore and thereby stops the eventual rupture of the outer mitochondrial membrane with the attendant cytosolic release of cytochrome *c* [38,39]. It will be interesting to determine whether similar rules apply to the ability of HK1 to block TNF-dependent cell death.

5. Conclusions

We demonstrate that loss of HK1 sensitizes a range of human cell lines to the pro-apoptotic functions of three different inducers of cell death and show that loss of HK1 results in increased mitochondrial membrane permeability. We expand on these findings to show that

loss of HK1 accelerates the TNF-responsive formation of complex II and thereby results in an accelerated activation of the apoptotic program. We consider it noteworthy that our primary screen did not identify any gene products that activate the pro-survival functions of HK1 as modifiers of TNF-dependent cell death (Supplementary Fig. S4). These observations show that HK1-dependent regulation of pro-apoptotic signals is mechanistically distinct to HK1-dependent regulation of pro-survival signals and implicate HK1 as a critical nexus in the integration of extrinsic signals that ultimately determine cell viability.

Acknowledgements

We are grateful to Dr. Kevin Kane and Dr. James Smiley for the critical reading of the manuscript. Brendon Parsons and Yanxin Zhong provided technical assistance with the NF- κ B reporter assay and Dr. Michele Barry provided the NF- κ B reporter assay plasmids. dsRNA libraries were generously provided by Dr. David Evans. Dr. Andrew Simmons provided assistance with confocal microscopy. This research was funded by a grant from the Canadian Institutes of Health Research (MOP 77746). EF is a Scholar of the Alberta Heritage Foundation for Medical Research and holds a Canada Research Chair in Innate Immunity.

Appendix A. Supplementary data

Supplementary data associated with this article can be found, in the online version, at doi:10.1016/j.cellsig.2010.04.010.

References

- [1] B.B. Aggarwal, *Nat. Rev. Immunol.* 3 (9) (2003) 745.
- [2] H. Wajant, K. Pfizenmaier, *Cell Death Differ.* 10 (1) (2003) 45.
- [3] G. Chen, *Science* 296 (5573) (2002) 1634.
- [4] M. Karin, *Nat. Immunol.* 3 (3) (2002) 221.
- [5] J. Kucharczak, M.J. Simmons, Y. Fan, *Oncogene* 22 (56) (2003) 8961.
- [6] J.L. Luo, H. Kamata, *J. Clin. Investig.* 115 (10) (2005) 2625.
- [7] S. Papa, C. Bubic, F. Zazzeroni, C.G. Pham, C. Kuntzen, J.R. Knabb, K. Dean, *Cell Death Differ.* 13 (5) (2006) 712.
- [8] O. Micheau, *Cell* 114 (2) (2003) 181.
- [9] C.K. Ea, L. Deng, Z.P. Xia, G. Pineda, *Mol. Cell* 22 (2) (2006) 245.
- [10] S. Ghosh, *Nature* 344 (6267) (1990) 678.
- [11] M. Karin, Y. Ben-Neriah, *Annu. Rev. Immunol.* 18 (2000) 621.
- [12] J.R. Muppidi, J. Tschopp, *Immunity* 21 (4) (2004) 461.
- [13] M.S. Sheikh, *Cell Cycle* 2 (6) (2003) 550.
- [14] Y. Shi, *Mol. Cell* 9 (3) (2002) 459.
- [15] E.E. Varfolomeev, M. Schuchmann, V. Luria, N. Chiannikulchai, J.S. Beckmann, I.L. Mett, D. Rebrikov, V.M. Brodianski, O.C. Kemper, O. Kollet, T. Lapidot, D. Soffer, T. Sobe, K.B. Avraham, T. Goncharov, H. Holtmann, P. Lonai, *Immunity* 9 (2) (1998) 267.
- [16] W.C. Yeh, J.L. Pompa, M.E. McCurrach, H.B. Shu, A.J. Elia, A. Shahinian, M. Ng, A. Wakeham, W. Khoo, K. Mitchell, W.S. El-Deiry, S.W. Lowe, D.V. Goeddel, *Science* 279 (5358) (1998) 1954.
- [17] C. Scaffidi, S. Fulda, A. Srinivasan, C. Friesen, F. Li, K.J. Tomaselli, K.M. Debatin, P.H. Krammer, *EMBO J.* 17 (6) (1998) 1675.
- [18] A. Thorburn, *Cell. Signal.* 16 (2) (2004) 139.
- [19] F. Balkwill, *Nat. Rev. Cancer* 9 (5) (2009) 361.
- [20] B.D. Parsons, A. Schindler, D.H. Evans, *PLoS ONE* 4 (12) (2009) e8471.
- [21] S. Abu-Hamad, H. Zaid, A. Israelson, E. Nahon, *J. Biol. Chem.* 283 (19) (2008) 13482.
- [22] M.J. Birnbaum, *Dev. Cell* 7 (6) (2004) 781.
- [23] N. Majewski, V. Nogueira, P. Bhaskar, P.E. Coy, J.E. Skeen, K. Gottlob, N.S. Chandel, C.B. Thompson, R.B. Robey, *Mol. Cell* 16 (5) (2004) 819.
- [24] N. Majewski, V. Nogueira, R.B. Robey, *Mol. Cell. Biol.* 24 (2) (2004) 730.
- [25] R.B. Robey, *Oncogene* 25 (34) (2006) 4683.
- [26] D. Bond, *PLoS Pathog.* 5 (11) (2009) e1000655.
- [27] D. Bond, D.A. Primrose, E. Foley, *Biol. Proced. Online* 10 (2008) 20.
- [28] T.D. Gilmore, *Cancer Treat. Res.* 115 (2003) 241.
- [29] F.R. Greten, *Cancer Lett.* 206 (2) (2004) 193.
- [30] A. Kumar, Y. Takada, A.M. Boriak, *J. Mol. Med.* 82 (7) (2004) 434.
- [31] A. Birmingham, E.M. Anderson, A. Reynolds, D. Ilesley-Tyree, D. Leake, Y. Fedorov, S. Baskerville, E. Maksimova, K. Robinson, J. Karpilow, W.S. Marshall, *Nat. Meth.* 3 (3) (2006) 199.
- [32] C.J. Echeverri, P.A. Beachy, B. Baum, M. Boutros, F. Buchholz, S.K. Chanda, J. Downward, J. Ellenberg, A.G. Fraser, N. Hacohen, W.C. Hahn, A.L. Jackson, A. Kiger, P.S. Linsley, L. Lum, Y. Ma, B. Mathey-Prevot, D.E. Root, D.M. Sabatini, J. Taipale, N. Perrimon, *Nat. Meth.* 3 (10) (2006) 777.
- [33] M.G. Vander Heiden, L.C. Cantley, C.B. Thompson, *Science* 324 (5930) (2009) 1029.
- [34] N. Shulga, R. Wilson-Smith, *Cell Cycle* 8 (20) (2009) 3355.
- [35] H. Azoulay-Zohar, A. Israelson, S. Abu-Hamad, *Biochem. J.* 377 (Pt 2) (2004) 347.
- [36] J.E. Wilson, *Rev. Physiol. Biochem. Pharmacol.* 126 (1995) 65.
- [37] J.G. Pastorino, N. Shulga, *J. Biol. Chem.* 277 (9) (2002) 7610.
- [38] F. Chiara, D. Castellaro, O. Marin, V. Petronilli, W.S. Brusilow, M. Juhaszova, S.J. Sollott, M. Forte, P. Bernardi, *PLoS ONE* 3 (3) (2008) e1852.
- [39] K.W. Kinnally, *Apoptosis* 12 (5) (2007) 857.